Table 2–2 *Average Chemical and Mineral Compositions of Selected Plutonic Rocks*

	Granite	Syenite	Granodiorite	Quartz Diorite	Diorite	Gabbro	Olivine Diabase	Diabase	Dunite	Lherzolite (Peridotite)
Chemical composition										
SiO_2	70.18	60.19	65.01	61.59	56.77	48.24	48.54	50.48	40.49	43.95
TiO_2	0.39	0.67	0.57	0.66	0.84	0.97	1.31	1.45	0.02	0.10
Al_2O_3	14.47	16.28	15.94	16.21	16.67	17.88	15.24	15.34	0.86	4.82
Fe_2O_3	1.57	2.74	1.74	2.54	3.26	3.16	3.06	3.84	2.84	2.20
FeO	1.78	3.28	2.65	3.77	4.40	5.95	8.88	7.78	5.54	6.34
MnO	0.12	0.14	0.07	0.10	0.13	0.13	0.21	0.20	0.16	0.19
MgO	0.88	2.49	1.91	2.80	4.17	7.51	8.08	5.79	46.32	36.81
CaO	1.99	4.30	4.42	5.38	6.74	10.99	9.38	8.94	0.70	3.57
Na_2O	3.48	3.98	3.70	3.37	3.39	2.55	2.69	3.07	0.10	6.63
K_2O	4.11	4.49	2.75	2.10	2.12	0.89	0.98	0.97	0.04	0.21
H_2O	0.84	1.16	1.04	1.22	1.36	1.45	1.35	1.89	2.88	1.08
P_2O_5	0.19	0.28	0.20	0.26	0.25	0.28	0.28	0.25	0.05	0.10
Density	2.667	2.757	2.716	2.806	2.839	2.976	2.970	2.965	3.289	3.330
Mineral composition										
Quartz	25	—	21	20	2	—	—	—	—	—
K Feldspar	40	72	15	6	3	—	—	—	—	—
Oligoclase	26	12	—	—	—	—	—	—	—	—
Andesine	—	—	46	56	64	—	—	—	—	—
Labradorite	—	—	—	—	—	65	63	62	—	—
Biotite	5	2	3	4	5	1	—	1	—	—
Amphibole	1	7	13	8	12	3	—	1	—	—
Orthopyroxene	—	—	—	1	3	6	—	—	2	15
Clinopyroxene	—	4	—	3	8	14	21	29	—	10
Olivine	—	—	—	—	—	7	12	3	95	71
Magnetite	2	2	1	2	2	2	2	2	2	1
Ilmenite	1	1	—	—	—	2	2	2	—	—
Apatite	tr	tr	tr	tr	tr	—	—	—	—	—
Sphene	tr	tr	1	tr	tr	—	—	—	—	—
Spinel	—	—	—	—	—	—	—	—	1	3

Source: After Daly and Larsen, *Geol. Soc. Am. Special Paper 36,* 1942 with modifications and reduced to 100%.

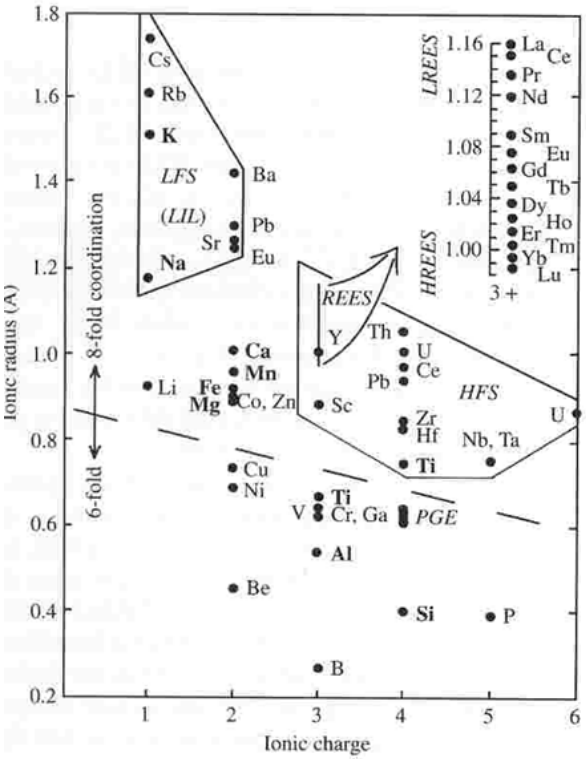

20 Radii and classification of positively charged ions of major (bold letters) and trace elements. Radii based on eightfold coordination in upper part of diagram and on sixfold in lower part. Rare earth elements **(REEs)** in center of diagram are plotted on an expanded scale in upper right. On the basis of **ionic potential** (charge/radius), most elements can be subdivided into two categories surrounded by polygons, namely, (1) Low field strength (LFS) elements, more commonly called **large-ion lithophile (LIL) elements,** in upper left; (2) **high-field-strength (HFS) elements** in right center. The lithophile designation arises from an affinity for silicate rocks, as contrasted with elements having an affinity for metallic phases (siderophile) containing Fe, Co, Ni, and so on, as in the core of the Earth, or for sulfide phases (chalcophile) containing S, Cu, Zn, and so on. Ionic potential also serves as a rough index of the **mobility** of cations of the elements, that is, their solubility in aqueous solutions; elements with low (<3) and high (>12) potential tend to be more soluble and mobile than elements in midrange. PGE, **platinum group elements** (Ru, Rh, Pd, Os, Ir, Pt). (Data from Shannon, 1976.)

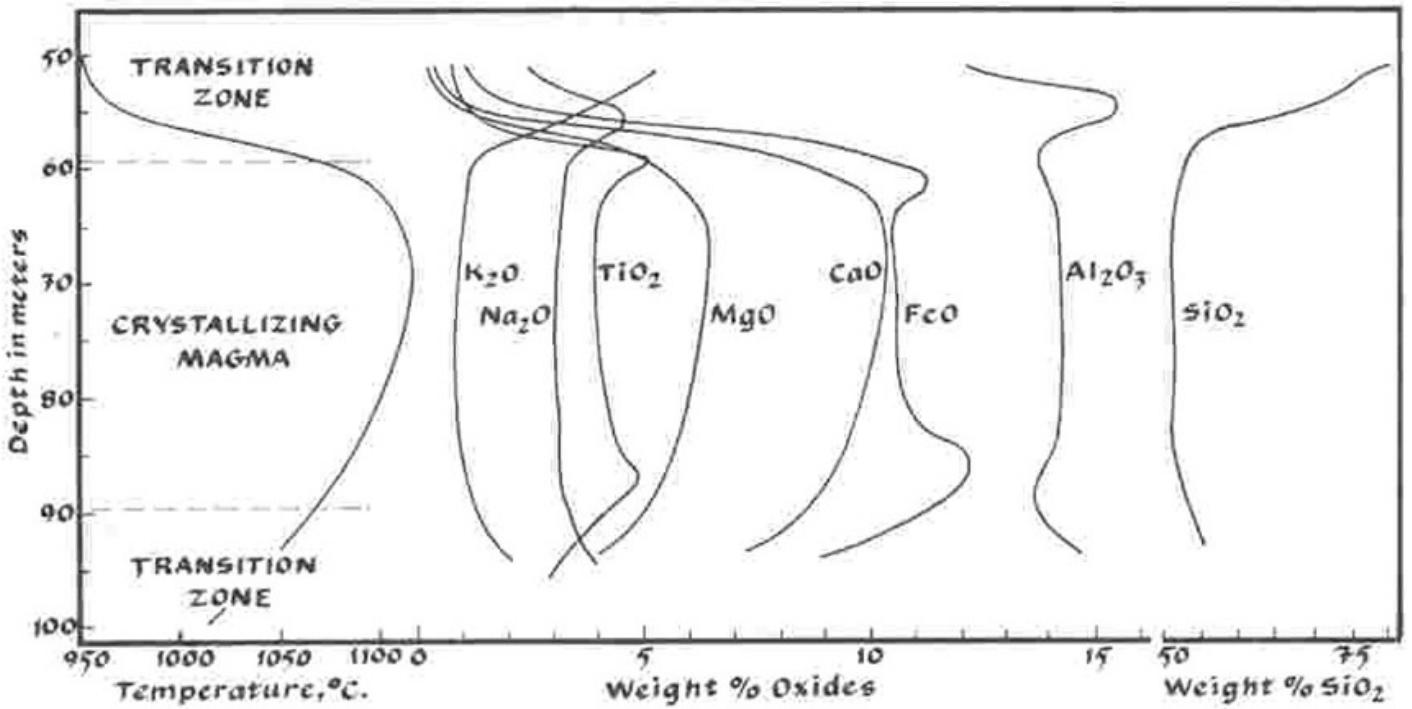

Figure 5–1 As the basaltic magma in the lava lake of Kilauea Iki solidified, the concentrations of the various components changed in response to progressive crystallization. The plot above shows the variations of several of these components in liquids (quenched to glass) in samples recovered by drilling into the crystallizing basalt. Note that some components are depleted from the liquid while others are enriched. The rates of enrichment or depletion depend on the compositions and proportions of crystallizing minerals. If the differentiated liquids were removed and allowed to crystallize elsewhere, they would form a series of rocks of different compositions. Without this second step of segregation, the process of differentiation is incomplete. (Data from W. C. Luth, Sandia Corporation, personal communication.)

Table 2.3 Generally Compatible Trace Elements and the Minerals in Which They Occur

Major Mineral	Simple Formula	Compatible Trace Elements
Olivine	$(Mg, Fe)_2SiO_4$	Ni, Cr, Co
Orthopyroxene	$(Mg, Fe)SiO_3$	Ni, Cr, Co
Clinopyroxene	$(Ca, Mg, Fe)_2(Si, Al)_2O_6$	Ni, Cr, Co, Sc
Hornblende	$(Ca, Na)_{2-3}(Mg, Fe, Al)_5$ $(Si, Al)_8O_{22}(OH, F)_2$	Ni, Cr, Co, Sc
Biotite	$K_2(Mg, Fe, Al, Ti)_6$ $(Si, Al)_8O_{20}(OH, F)_4$	Ni, Cr, Co, Sc, Ba, Rb
Muscovite	$K_2Al_4(Si, Al)_8O_{20}(OH, F)_4$	Rb,Ba
Plagioclase	$(Na, Ca)(Si, Al)_4O_8$	Sr, Eu
K-feldspar	$KAlSi_3O_8$	Ba, Sr, Eu
Accessory Minerals[a]		
Magnetite	Fe_3O_4	V, Sc
Ilmenite	$FeTiO_3$	V, Sc
Sulfides		Cu, Au, Ag, Ni, PGE[b]
Zircon	$ZrSiO_4$	Hf, U, Th, heavy REEs
Apatite	$Ca_5(PO)_3(OH, F, Cl)$	U, middle REEs
Allanite	$Ca_2(Fe, Ti, Al)_3(O, OH)$ $(Si_2O_7)(SiO_4)$	Light REEs, Y, U, Th
Xenotime	YPO_4	Heavy REEs
Monazite	$(Ce, La, Th)PO_4$	Y, light REEs
Titanite (sphene)	$CaTiSiO_5$	U, Th, Nb, Ta, middle REEs

[a]Accessory minerals constitute only a small fraction of rock but their very high partition coefficients create a disproportionate influence on bulk distribution coefficients.

[b]**Platinum group elements:** Ru, Rh, Pd, Os, Ir, Pt.

Table 2.4 Trace Elements Substituting for Major Elements of Similar Ionic Size and Charge (see Figure 2.20)

Major Element	Substituting Trace Element(s)
Si	Ge, P
Ti	V
Al	Ga
Fe	Cr, Co, Ni
Mg	Cr, Co, Ni
Ca	Sr, Eu, REEs
Na	Eu
K	Rb, Ba, Sr, Eu

Table 2.5 Partition Coefficients for Some Trace Elements

	U	Rb	K	Ba	Sr	Yb	Y	Nb	Eu	La	Ce	Zr	Ti	V	Cr	Ni
BASALT MAGMA																
Plagioclase	0.01	0.07	0.17	0.23	1.83	0.067	0.03	0.01	0.34	0.19	0.1	0.048	0.04			
Clinopyroxene	0.04	0.031	0.038	0.026	0.06	0.62	0.9	0.005	0.51	0.056	0.09	0.1	0.4	1.35	34	1.5–14
Orthopyroxene		0.022	0.014	0.013	0.04	0.34	0.18	0.15	0.05		0.02	0.18	0.1	0.6	10	5
Olivine	0.002	0.01	0.007	0.01	0.014	0.014	0.01	0.01	0.007	0.007	0.006	0.012	0.02	0.06	0.7	6–29
Magnetite						1.5	0.2	0.4	1.0	2.0	2.0	0.1	7.5	26	153	29
Garnet		0.042	0.015	0.023	0.012	11.5	9	0.02	0.49	0.01	0.03	0.65	0.3		2	
RHYOLITE MAGMA																
Plagioclase	0.093	0.041	0.1	0.31	4.4	0.09	0.1	0.06	2.1	0.38	0.27	0.1	0.05			
K-feldspar	0.02	0.5		4.3	3.76	0.0015			2.6	0.07	0.04	0.03				
Quartz	0.025	0.04	0.013	0.022		0.017			0.056	0.015	0.014		0.038			
Biotite	0.167	4.2		5.4	0.5	0.54			0.87	3.18	0.3				5.2	
Hornblende		0.014	0.08	0.044	0.022	8.38	6	4	5.14		1.5	4	7			
Zircon	340					527			16	17	17				190	
Apatite						24	40	0.1	30	14.5	35	0.1	0.1			
Allanite	15.5					31			111	2595	2279			15.5	380	
Titanite								6.3		4						

Data from Rollinson, 1993.

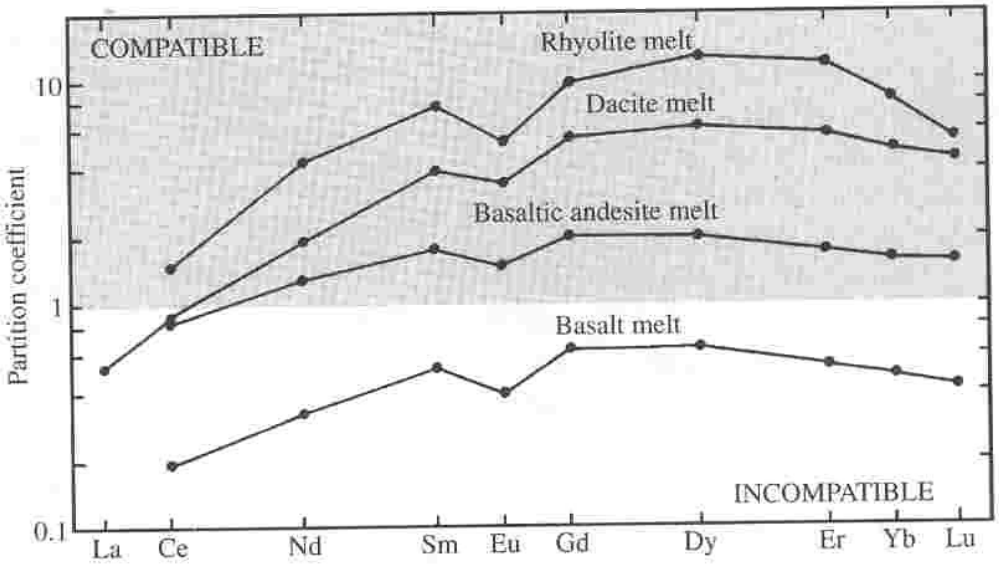

2.21 Partition coefficients for REEs between amphibole and indicated melts. REEs are more compatible in more silicic and lower-T melts. (Redrawn from Rollinson, 1993.)

Table 2.6 Trace Element Characteristics Useful in Evaluating Petrogenesis of Rocks

Element	Characteristics and Interpretations
Ni, Co, Cr	Typically highly compatible elements. High concentrations (e.g., Ni = 250–300 ppm, Cr = 500–600 ppm) of these elements indicate derivation of parental magmas from a peridotite mantle source. Declining concentrations of Ni and to a lesser extent Co in a rock series suggest olivine fractionation. Decrease in Cr suggests spinel or clinopyroxene fractionation.
PGE, Cu, Au, Ag	Strongly partitioned into immiscible sulfide melts. A series of mafic magmas that lack sulfides may show increases in these elements. In most other magma series, these are compatible elements that decline with increasing silica.
V, Ti	Typically compatible elements in ilmenite and titanomagnetite, although Ti can become enriched in some mafic magmas that lack these oxide minerals.
Nb	Incompatible element in most magmas. However, because it substitutes somewhat for Ti, residual titanates (such as rutile) may cause depletions of Nb in subduction-zone magma sources. Nb has a lower solubility in aqueous fluids than other equally incompatible elements.
Zr, Hf	Characteristically incompatible in mafic magmas and not readily substituting in mantle phases. In zircon-saturated (silicic) magmas both may behave as compatible elements.
P	Characteristically incompatible in mafic magmas but becomes a compatible element in intermediate and silicic magmas where apatite is a stable phase.
Ba	Substitutes for K in micas, K-feldspar, and to a lesser extent amphibole. A change from incompatible to compatible behavior in a magma series may indicate an increasing role for one of these phases.
Rb	Incompatible element in most magma, but it substitutes for K in micas and K-feldspar in silicic magmas, though not as strongly as Ba.
Sr, Eu	Substitute readily for Ca in plagioclase and K in K-feldspar. Declining Sr concentrations indicates feldspar removal from a series of related magmas. Sr is more incompatible under mantle conditions because of the absence of feldspar.
REEs	Generally, the *trivalent* rare earth elements are incompatible in basaltic magmas. Garnet more readily accommodates heavy REEs than light REEs and a steep REE pattern may indicate garnet remained in a mantle residue. Titanite prefers the middle REEs. Apatite, monazite, and allanite have very high partition coefficients for light REEs; consequently, light REEs are commonly compatible elements in rhyolitic magmas that have these minerals. Zircon and xenotime prefer heavy REEs but their abundance in natural magmas is rarely sufficient to make the heavy REEs behave as compatible elements.
Y	Generally behaves incompatibly, as do middle to heavy REEs. It has a high partition coefficient in garnet and to a lesser extent in amphibole. Its behavior is strongly affected by REE-rich accessory minerals such as apatite and especially xenotime.

Data from Green (1989).

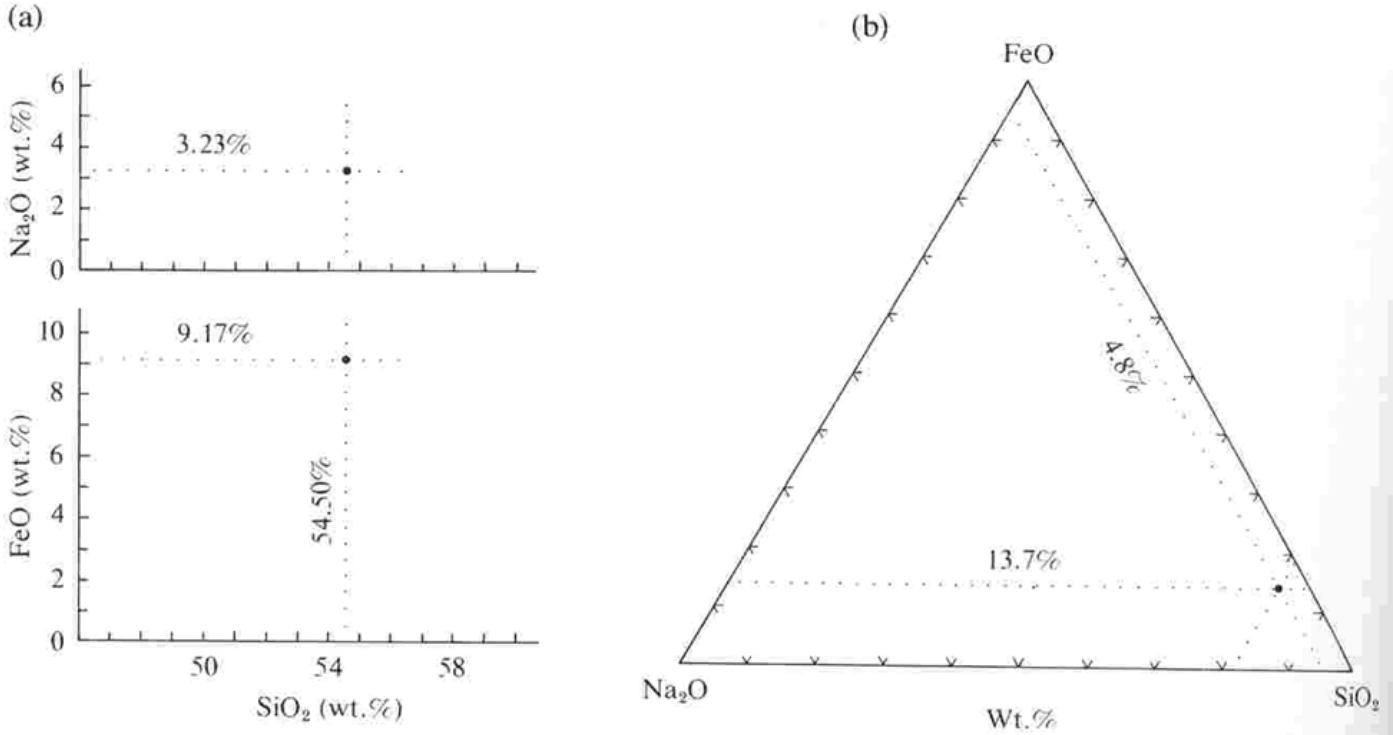

2.3 Plotting compositional data on **variation diagrams.** A sample contains 9.17 wt.% FeO, 3.23 wt.% Na_2O, and 54.50 wt.% SiO_2. In the Cartesian diagram (a), FeO and Na_2O are plotted against SiO_2 (all in wt.%). To plot SiO_2, Na_2O, and FeO on the triangular diagram (b), *they must be recalculated to total 100.00.* First, they are summed, 54.50 + 9.17 + 3.23 = 66.90 and a recalculation multiplier found, 100.00/66.90 = 1.495. Second, the wt.% of each constituent is recalculated; Si_2O is 54.50 × 1.495 = 81.48, FeO = 13.71, and Na_2O = 4.83. The total of the three recalculated oxides is now 81.5 + 13.7 + 4.8 = 100.0 These recalculated values can then be plotted so that each apex represents 100 wt.% of a constituent and the leg of the triangle opposite the apex is the locus of points representing 0 wt.% of that constituent. A line parallel to the leg of the triangle opposite the FeO apex and 13.7% of the way toward that apex is the locus of points representing 13.7 wt.% FeO. Similarly, the line labeled 4.8 % is the locus of points representing 4.8 wt.% Na_2O. The intersection of these two lines is a point that represents the relative SiO_2, FeO, and Na_2O wt.% in the sample. Note that it is only necessary to draw lines for any two of the three constituents represented in the diagram because the third variable is the difference from 100% of the other two.

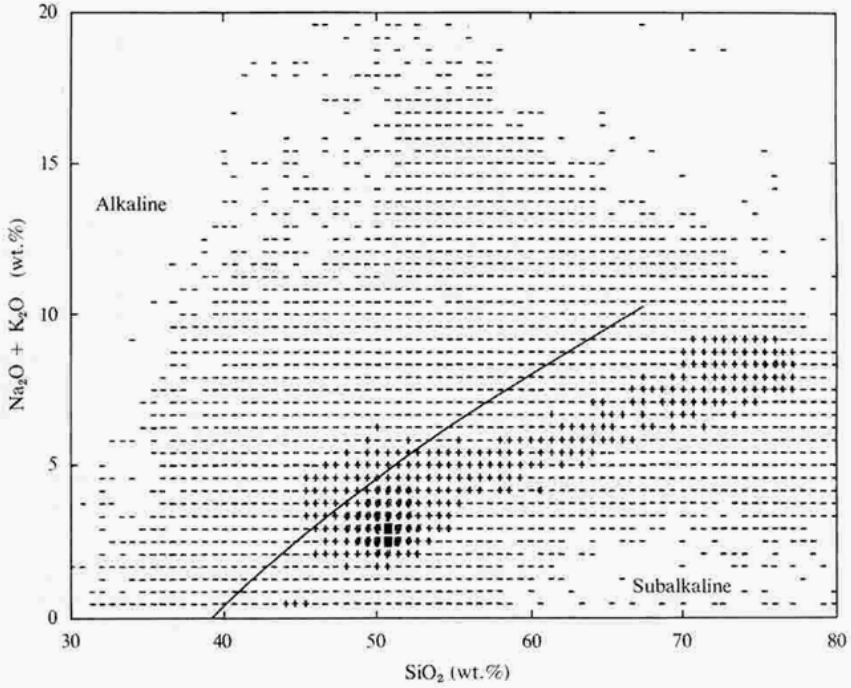

	Upper limit of analyses	Total analyses	Analyses as %
-	41	19,207	46.73
+	116	15,626	38.02
♦	330	5,449	13.25
■	462	820	2.00
	Total	41,102	100.00

2.4 Chemical analyses of over 41,000 igneous rocks from around the world of all ages. Each symbolized plotted point represents a particular number of analyses falling within the indicated range (0–41, 42–116, etc.). Nearly half (46.7%) of all igneous rocks are widely scattered over the diagram (dash symbol), whereas slightly more than half (53.3%) are tightly clustered in a central band. Note the still higher concentration of analyses near 2.5 wt.% ($Na_2O + K_2O$) and 50 wt.% SiO_2, corresponding roughly to basalt, the dominant magmatic rock type on Earth. (Compiled by and furnished courtesy of R. W. Le Maitre, University of Melbourne, Australia.)

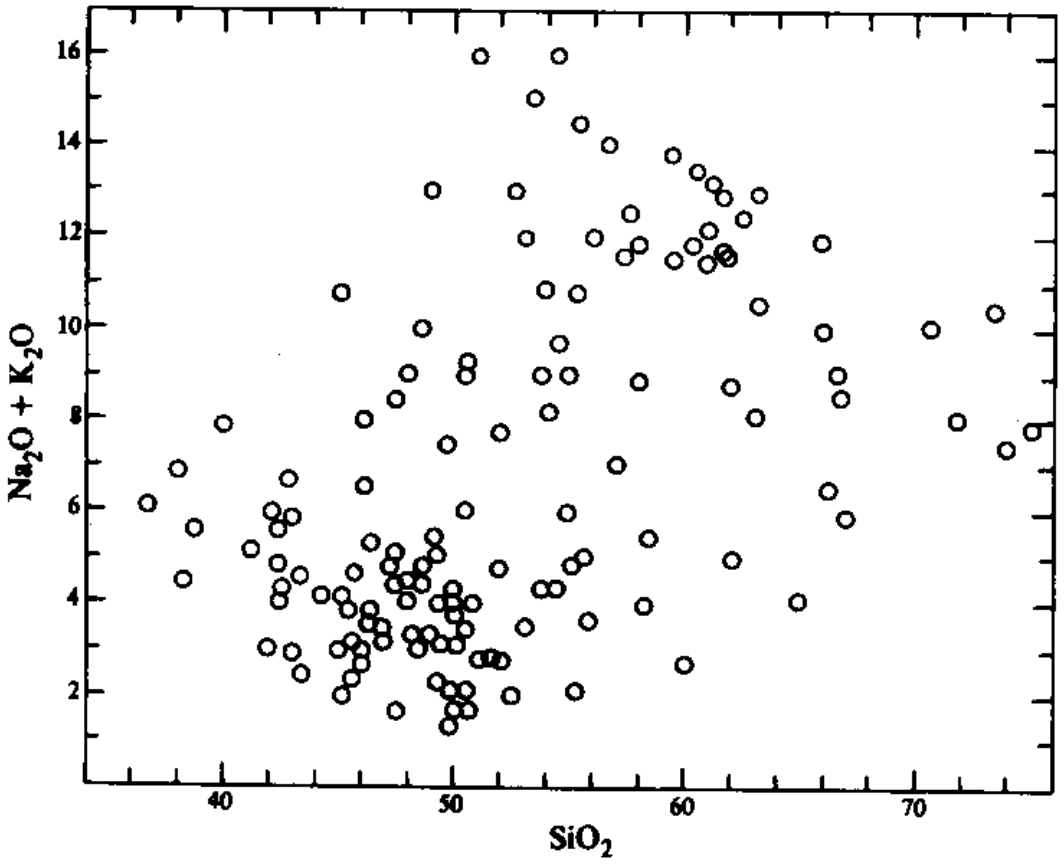

Figure 2.1 Plot of total alkalis versus silica for a wide selection of volcanic rocks (data from Carmichael, Turner & Verhoogen 1974).

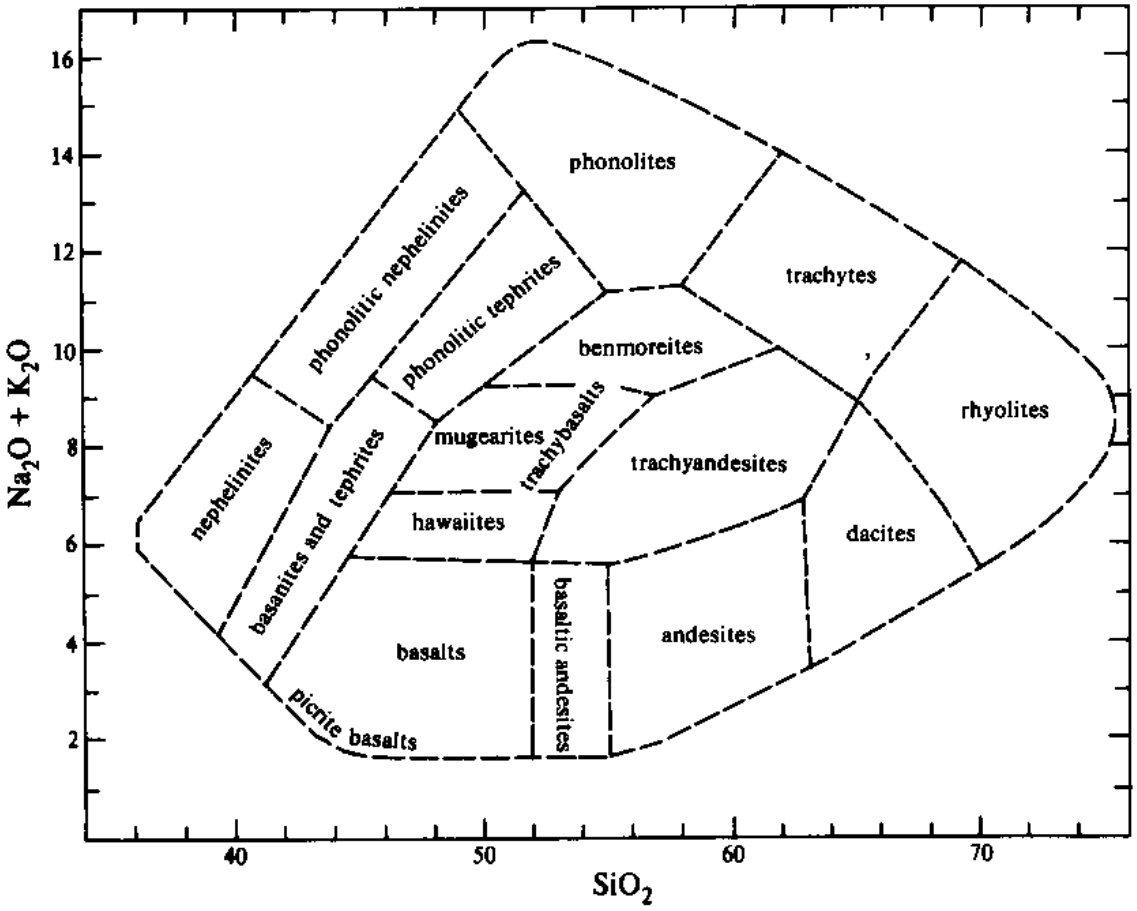

Figure 2.2 Nomenclature of normal (i.e. ~~non-potassic~~) volcanic rocks. The boundaries are not intended to be sharp, the fields labelled being intended only to show the approximate areas in which different types plot. For the nomenclature of equivalent potassic types, see Table 2.1.

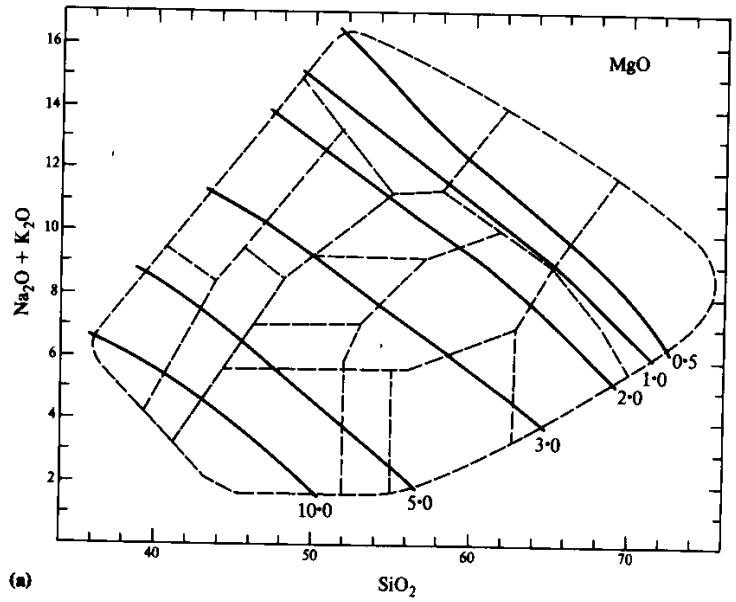
MgO
$Na_2O + K_2O$
SiO_2
16
14
12
10
8
6
4
2
40
50
60
70
0·5
1·0
2·0
3·0
5·0
10·0

(a)

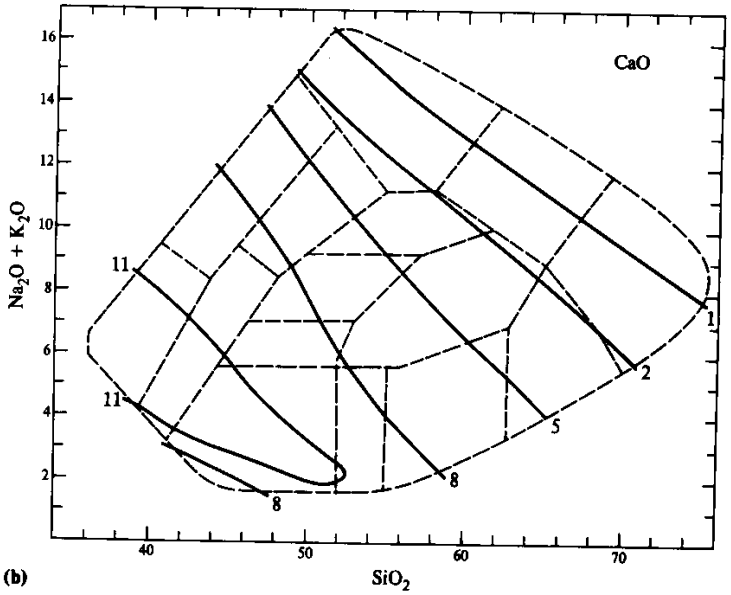
CaO
$Na_2O + K_2O$
SiO_2
16
14
12
10
8
6
4
2
40
50
60
70
11
11
1
2
5
8
8

(b)

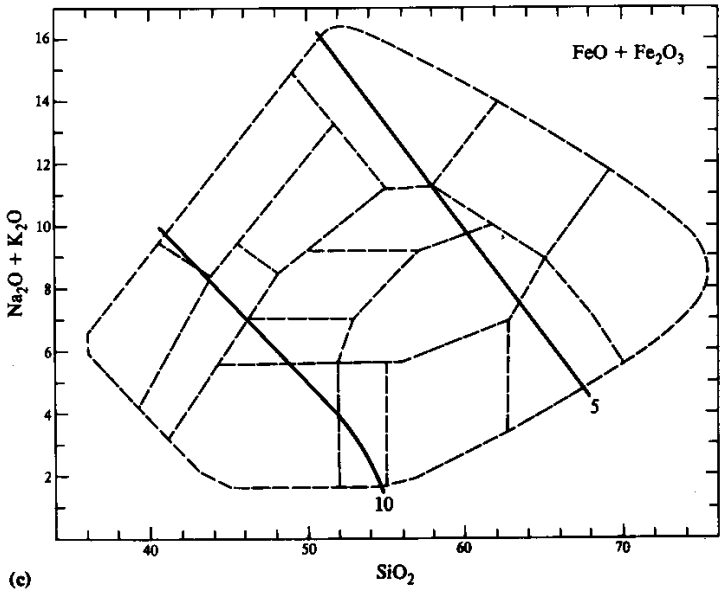
FeO + Fe2O3
Na2O + K2O
SiO2
16
14
12
10
8
6
4
2
40
50
60
70
5
10

(c)

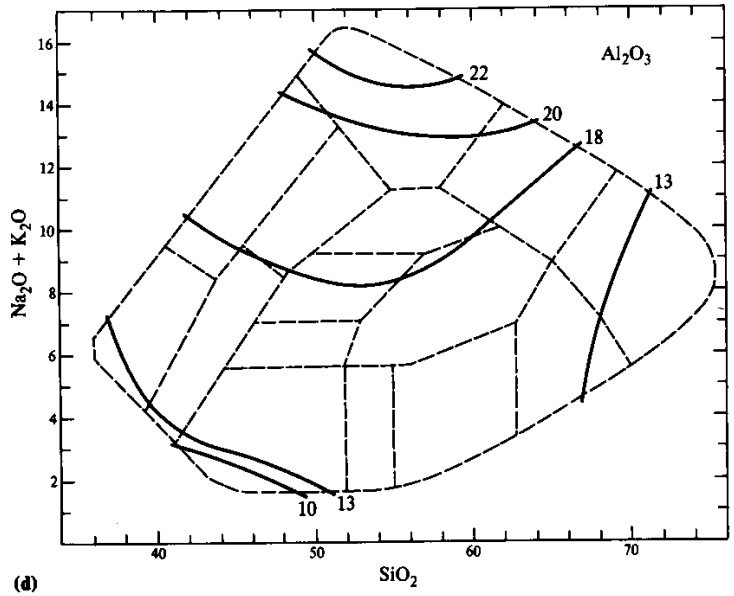
Al2O3
Na2O + K2O
SiO2
16
14
12
10
8
6
4
2
40
50
60
70
22
20
18
13
10
13

(d)

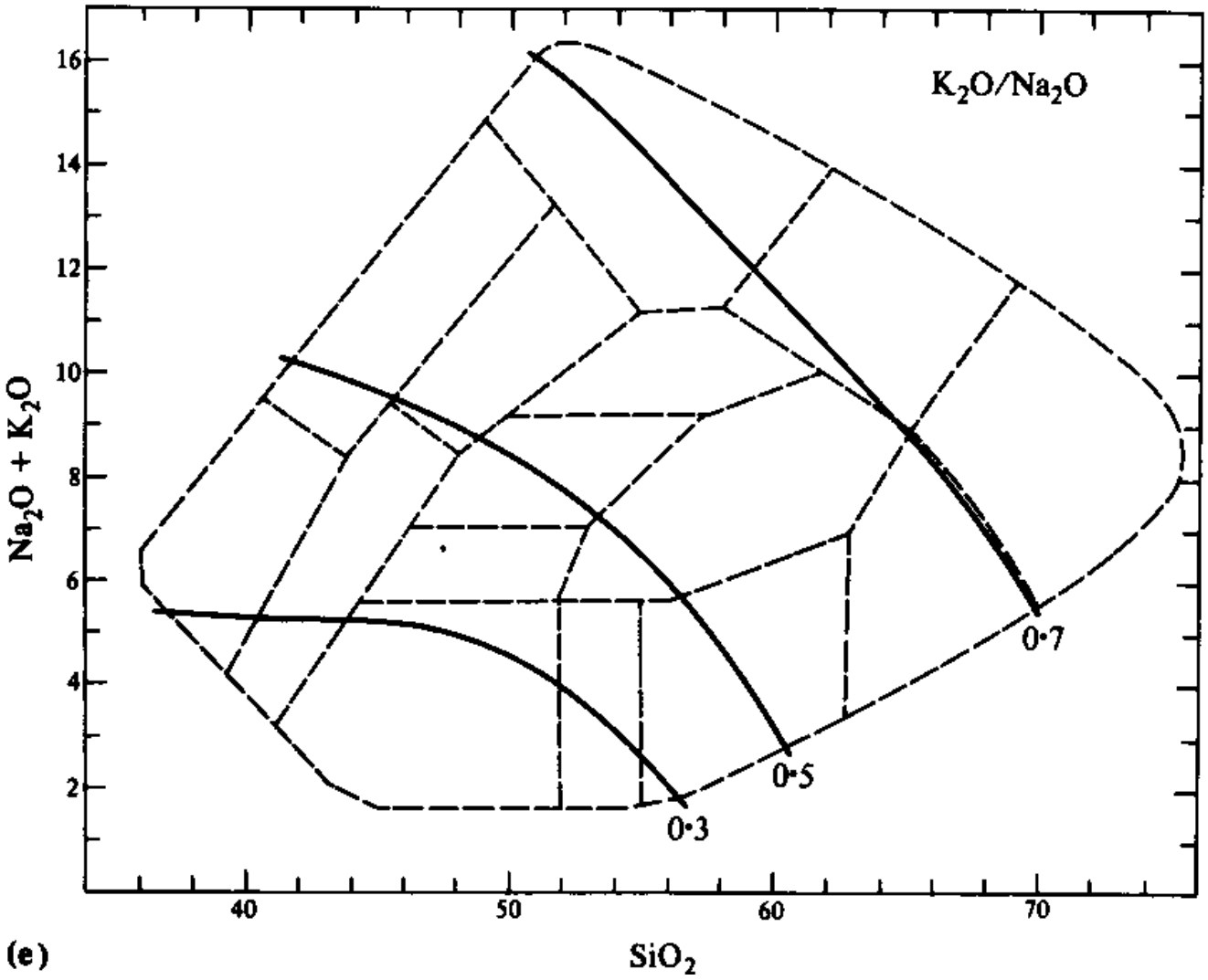

(e)

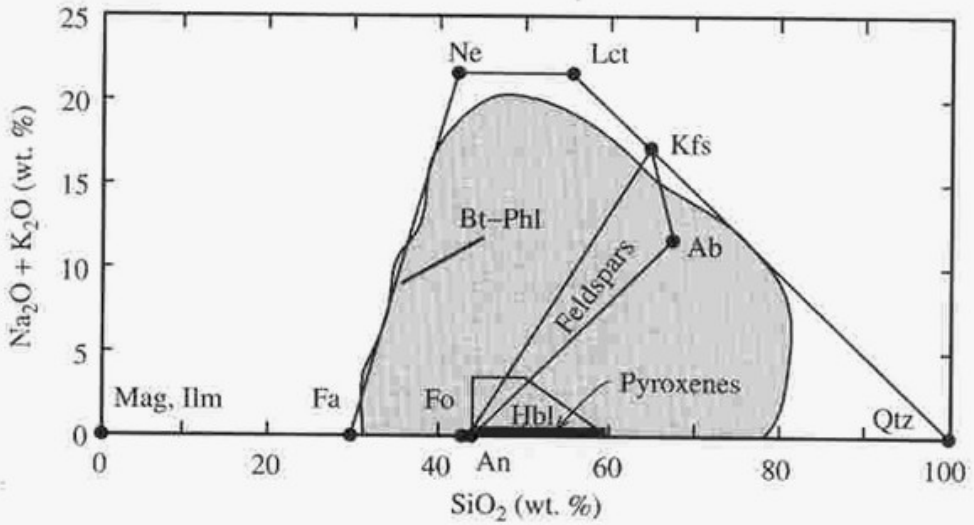

Ab	Albite	Ilm	Ilmenite
An	Anorthite	Kfs	K-feldspar
Bt	Biotite	Lct	Leucite
Fa	Fayalite	Mag	Magnetite
Fo	Forsterite	Ne	Nepheline
Hbl	Hornblende	Phl	Phlogopite
		Qtz	Quartz

2.5 End-member compositions of major magmatic rock-forming minerals compared with the field of worldwide magmatic rocks (shaded) from Figure 2.4. Triangular field of feldspar solid solution is outlined by the K-feldspar-albite-anorthite end members. Trapezohedral field is hornblende solid solutions.

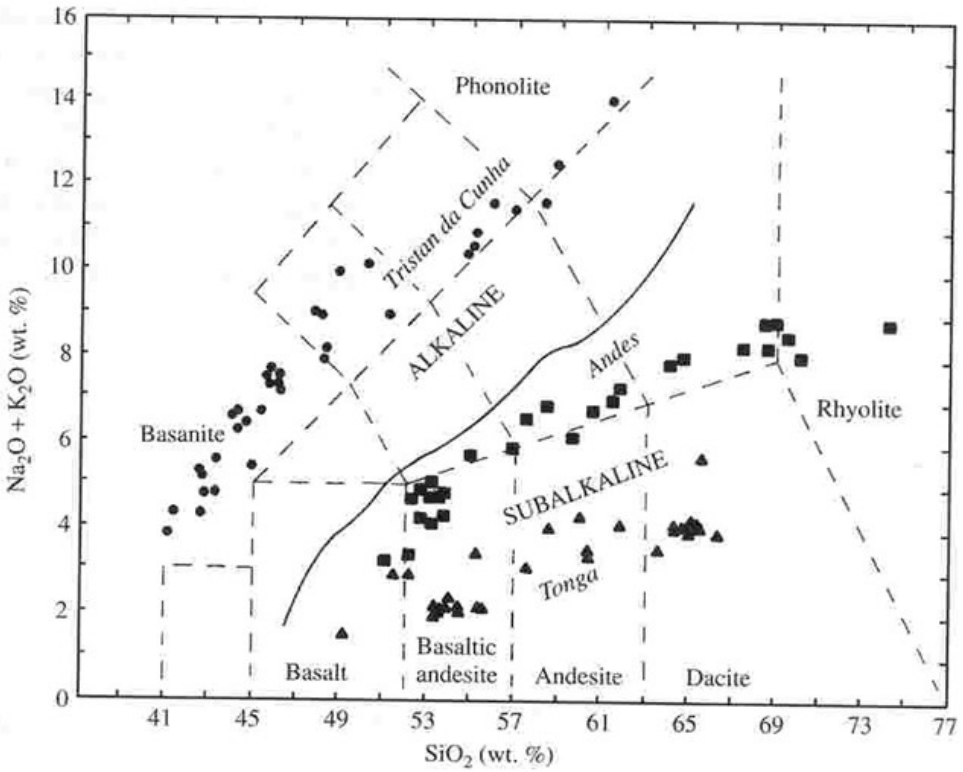

2.16 Total alkalies-silica diagram showing fields and examples of **subalkaline** and **alkaline rock suites.** Irregular solid line separates the field of nepheline-normative rocks from rocks having no normative nepheline in the 15,164-sample database of Le Bas et al., (1992). Light dashed lines delineate the IUGS volcanic rock-type classification from Figure 2.12. Note that a single rock type, such as basalt, can be either alkaline (*Ne*-normative) or subalkaline (*Hy*-normative). The alkaline volcanic suite of basanite, phonotephrite, tephriphonolite, and phonolite (filled circles) is from Tristan da Cunha, a volcanic oceanic island near the intersection of the Mid-Atlantic and Walvis Ridges in the South Atlantic Ocean (Le Roex et al., 1990). The subalkaline volcanic suite from the oceanic island arc of Tonga (filled triangles) is mostly basaltic andesite, andesite, and dacite (Cole, 1982). Subalkaline-suite rocks from Volcan Descabezado Grande and Cerro Azul in the southern volcanic zone of the Andes in central Chile (filled squares) are mostly basaltic andesite, trachyandesite, trachydacite, and rhyolite (Hildreth and Moorbath, 1988).

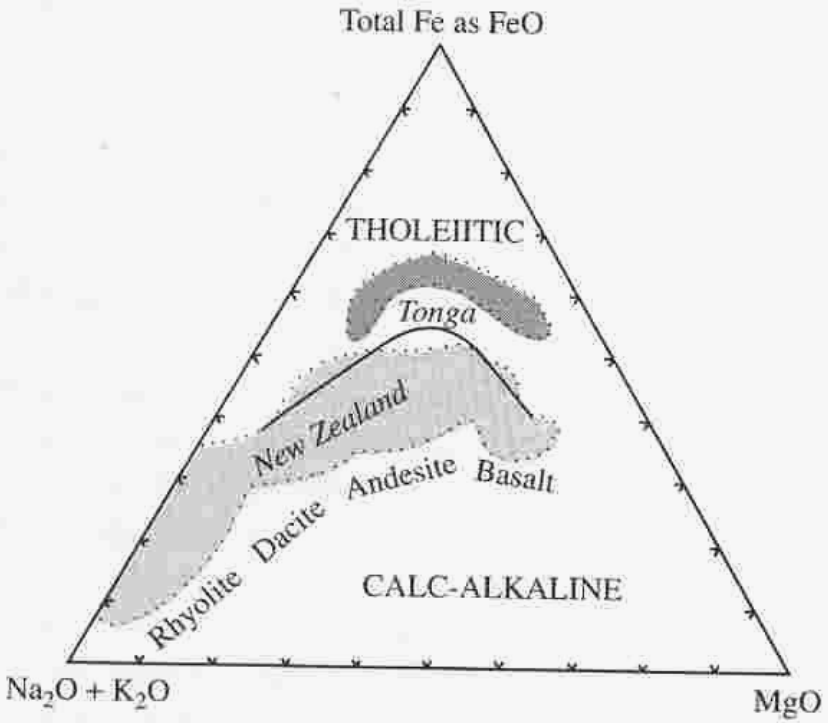

2.17 Subalkaline rocks can be subdivided into **tholeiitic** and **calc-alkaline rock suites. AFM diagram** in terms of alkalies ($Na_2O + K_2O$), total Fe as FeO, and MgO. Solid line separates fields of tholeiitic rocks, exemplified by volcanic rocks from the Tonga island arc in the Pacific Ocean (Figure 2.16), from calc-alkaline rocks, exemplified by most of the volcanic rocks from the North Island of New Zealand. Approximate range of rhyolite, dacite, andesite, and basalt rock types in New Zealand is indicated. Data from Cole (1982).

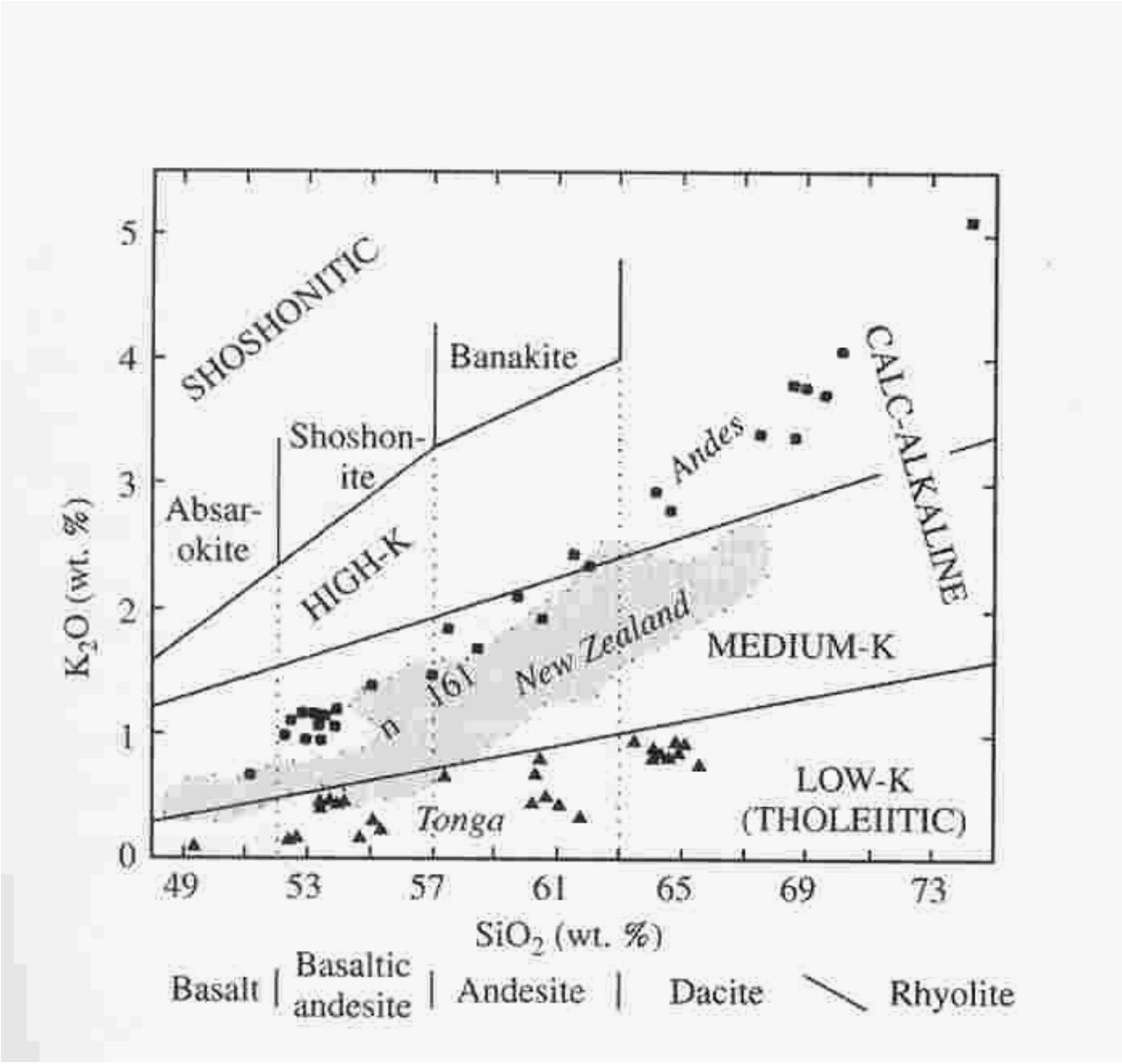
SHOSHONITIC
Banakite
Shoshon-
ite
Absar-
okite
HIGH-K
Andes
CALC-ALKALINE
MEDIUM-K
New Zealand
n
161
Tonga
LOW-K
(THOLEIITIC)
K_2O (wt. %)
SiO_2 (wt. %)
0
1
2
3
4
5
49
53
57
61
65
69
73
Basalt
Basaltic andesite
Andesite
Dacite
Rhyolite

Table 2.7 Element Concentration (ppm) in Chondrite, Primitive Mantle, and Normal Mid–Ocean Ridge Basalt (N-MORB)

	CHONDRITE	PRIMITIVE MANTLE	N-MORB
Rb	2.32	0.635	0.56
Ba	2.41	6.989	6.3
Th	0.029	0.085	0.12
U	0.008	0.021	0.047
Nb	0.246	0.713	2.33
Ta	0.014	0.041	0.132
K	545	250	600
La	0.237	0.687	2.5
Ce	0.612	1.775	7.5
Sr	7.26	21.1	90
P	1220	95	510
Nd	0.467	1.354	7.3
Sm	0.153	0.444	2.63
Zr	3.87	11.2	74
Hf	0.1066	0.309	2.05
Eu	0.058	0.168	1.02
Ti	445	1300	7600
Gd	0.2055	0.596	3.68
Tb	0.0374	0.108	0.67
Dy	0.254	0.737	4.55
Y	1.57	4.55	28
Ho	0.0566	0.164	1.01
Er	0.1655	0.48	2.97
Tm	0.0255	0.074	0.456
Yb	0.17	0.493	3.05
Lu	0.0254	0.074	0.455

Data from Sun and McDonough (1989).

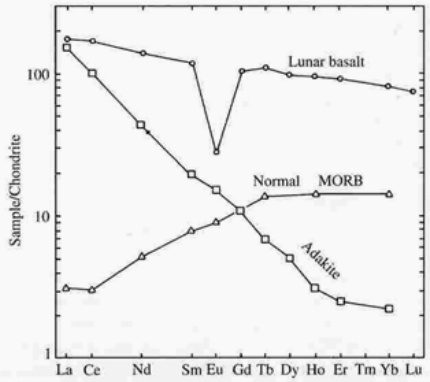

2.23 Very different **chondrite-normalized REE patterns** in three rocks. Compare patterns of partition coefficients in Figure 2.22, especially the mirror image of lunar basalt and plagioclase and of adakite and garnet.